

Interaction of Oxygen and Carbon Monoxide with CsAu Surfaces

A. F. Carley, M. W. Roberts,* and A. K. Santra

Department of Chemistry, University of Wales, Cardiff CF1 3TB, U.K.

Received: June 2, 1997; In Final Form: August 8, 1997[®]

The formation of cesium–gold alloys by the deposition of cesium on to a Au(100) surface has been investigated by both core-level (X-ray induced) and valence-level (He(II) radiation) spectroscopies. The stoichiometries of the alloy overlayer indicate the preferential segregation of cesium to the surface of the thinner films. Oxygen chemisorption generates three distinct oxygen species $O^{2-}(a)$, $O^{\delta-}(a)$, and $O_2^{\delta-}(a)$ characterized by their O(1s) binding energies and is accompanied by dealloying. With increasing oxygen exposure, the peroxo species is the major one present at 298 K. Dealloying is temperature dependent and is not complete at 80 K. Two of the oxygen states, $O^{\delta-}(a)$ and $O_2^{\delta-}(a)$, are reactive to carbon monoxide, forming carbonate species. Peroxo-type species are also formed readily by oxidation of pre-carbonated surfaces. The products formed from CO–O₂ mixtures depend on the mixture composition: with a 3:1 (CO:O₂) mixture at 298 K, O^{2-} , $O_2^{\delta-}$, and CO₃ species are observed, while for very much richer CO-mixtures (60:1) only O^{2-} and CO₃ species form; at 80 K both mixtures result in only peroxo ($O_2^{\delta-}$) and carbonate species.

Introduction

There has been intense interest in both the role of alkali metals as modifiers in heterogeneous catalysis^{1,2} and also the chemistry of the alkali metals themselves, including the formation of alloys and in particular CsAu. Recently we have explored the surface chemistry of multilayers of cesium deposited on to a Ni(110) surface³ using X-ray photoelectron spectroscopy (XPS) and also of cesium modified Cu(110) surfaces.² We have in the main been interested in oxygen states generated during oxygen chemisorption and their reactivity to carbon monoxide, carbon dioxide, and hydrocarbons (ethene and propene). In this paper we investigate multilayers of cesium present at a Au(100) surface, the thermally induced formation of Cs–Au alloys and the reactivity of such surfaces. There have been previous studies of Cs–Au films present at surfaces of Ru(001),^{4–6} Au(100),⁷ and polycrystalline gold,⁸ with evidence discussed for the formation of Cs–Au alloys. The bulk alloy is unstable in air and is thus not amenable to surface spectroscopic studies. The oxidation of cesium leads to various sub-oxides (the existence of which was first established by Simon⁹) and different states of oxygen, such as O_2^{2-} , O^{2-} , and O_2^- . However, it is the surface chemistry of the Cs–Au alloy, its thermal stability, and its chemisorption behavior to dioxygen, carbon monoxide, and carbon monoxide–dioxygen mixtures, that is the main impetus for this work. There have been no previous studies of either the chemisorption of carbon monoxide or the reactivity of carbon monoxide–dioxygen mixtures at CsAu alloy surfaces. The study of mixtures also allow us to comment on whether different reaction pathways operate under carbon monoxide-rich or oxygen-rich conditions. This approach has been particularly fruitful¹⁰ in highlighting the diverse chemistry associated with isolated oxygen adatoms, oxygen transient states, both molecular and atomic, in a wide range of catalytic oxidation systems. The stoichiometry of the Cs–Au overlayer present during CO chemisorption and oxidation is also investigated.

Experimental Section

The Au(100) crystal was cleaned by cycles of argon ion bombardment and annealing at 600 K, until impurity levels were below detection limits (<5% monolayer).

The core-level spectra were obtained with a VG Scientific UHV photoelectron spectrometer using a pass energy of 50 eV and Al K α radiation (1486.6 eV), resulting in a total instrumental energy resolution of 1.4 eV. Binding energies were calibrated against the Au(4f) peak at 84.0 eV. Valence level spectra were also recorded using He(II) radiation (40.8 eV) and an instrumental resolution of 1.0 eV. Spectral analysis and the calculation of the concentration of surface species has been described elsewhere.^{11,12} Spectroscopically pure gases from P. J. Mason were purified further by passing through cold traps (80 K) and cesium was evaporated from a well-degassed (SAES) getter.

Results and Discussion

Characterization of CsAu Films and Their Thermal Stability. In Figure 1 He(II), Au(4f), and Cs(3d) spectra are reported for Cs–Au overlayers of three film thicknesses, 3.2, 5.0, and 25 Å; these are compared with the spectra for the atomically clean Au(100) surface. Alloy film thicknesses are calculated from the attenuation of the pure metallic gold Au(4f) signal (obtained from a curve-fit analysis of the Au(4f) spectra) relative to the intensity from the clean Au(100) crystal. The mean free path (mfp) of photoelectrons through the alloy is calculated using the mfp values for the pure gold and cesium and the stoichiometry of the alloy.¹²

The alloy films were formed by in situ deposition of cesium on to a clean Au(100) surface at 298 K, conditions under which it has been reported that Cs diffuses into the gold subsurface to give an alloy where the Cs:Au ratio is 1:1.^{6–8} We shall consider the stoichiometry of the alloy layer shortly.

In the Au(4f) spectra we observe the emergence with increasing cesium deposition of shifted components at 85.3 and 89.1 eV due to the formation of an alloy overlayer. Eventually these components dominate the Au(4f) region. The binding energy of the Cs(3d_{5/2}) peak characteristic of the 25 Å “CsAu” overlayer is at 726.7 eV. In the He(II) spectra, there is a decrease in the Au(5d) band splitting with increasing film thickness, approaching a value of 1.5 eV for the thick (25 Å) film. The Au(4f) and Cs(3d) binding energies, as well as the observed Au(5d) splitting, are in agreement with previous studies on CsAu films.^{7,8}

The stoichiometries (Cs:Au) of the three Cs–Au alloy films, calculated from the curve-fitted intensities of the Au(4f)

[®] Abstract published in *Advance ACS Abstracts*, November 1, 1997.

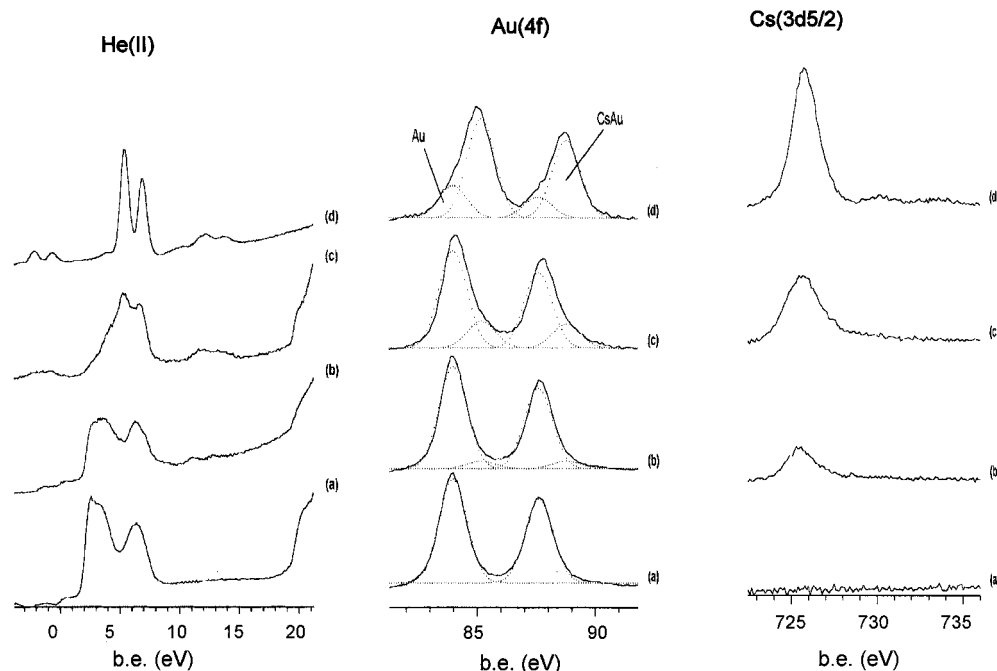


Figure 1. He(II), curve-fitted Au(4f) and Cs(3d_{5/2}) spectra of different CsAu film thicknesses (d_{CsAu}) at 298 K: (a) $d_{\text{CsAu}} = 0$, (b) $d_{\text{CsAu}} = 3.2$ Å, (c) $d_{\text{CsAu}} = 5.0$ Å, (d) $d_{\text{CsAu}} = 25$ Å.

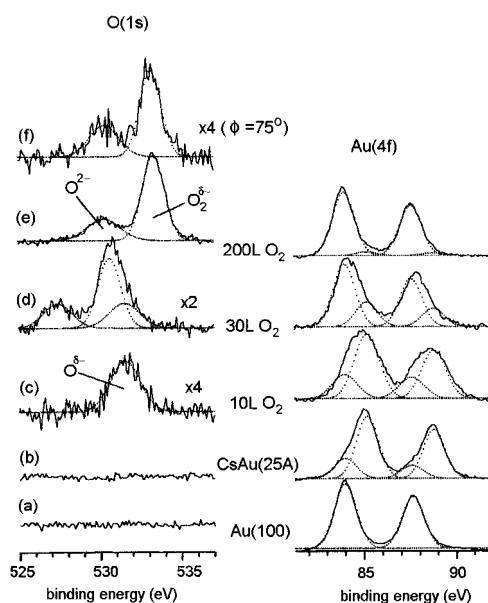


Figure 2. Curve-fitted O(1s) and Au(4f) spectra for a CsAu film ($d_{\text{CsAu}} = 25$ Å) exposed to oxygen at 298 K. The O(1s) spectrum f was recorded at a takeoff angle (with respect to the surface normal) $\phi = 75^\circ$ after 200 langmuir O₂ exposure. The peroxo species is dominant at high exposures.

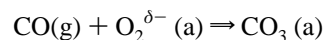
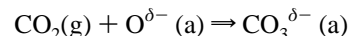
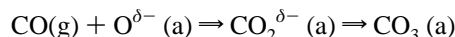
components arising from the pure gold and the alloy, were 2.2:1 (3.2 Å), 1.8:1 (5 Å), and 1:1 (25 Å), suggesting that for the thinner films there was an excess of cesium present at the surface of the "alloy", as reported by Wertheim et al.⁷ The homogeneity of the thick alloy films was examined by variable angle X-ray photoelectron studies and is discussed later.

Oxygen Chemisorption at 298 K. Figure 2 shows the development of the O(1s) and Au(4f) spectra of a thick (25 Å) CsAu alloy film as a function of oxygen exposure at 298 K. At low oxygen exposure (10 langmuir)¹⁶ the O(1s) intensity is mainly at 531.6 eV and is assigned to O^{δ-} species i.e. oxygen adatoms that have not developed the full ionic charge (2e) associated with an oxidic species. The latter can only be achieved through a contribution from the Madelung term

associated with the development of a "true oxide" state. With increasing oxygen exposure (30 langmuir) two further O(1s) features emerge, one at 530.6 eV (obtained via a curve-fit analysis) and the other at 527.4 eV. Analysis of each of these components gives the following concentrations of species 527.4 eV ($0.41 \times 10^{15} \text{ cm}^{-2}$); 530.6 eV ($0.87 \times 10^{15} \text{ cm}^{-2}$); and 531.6 eV ($0.41 \times 10^{15} \text{ cm}^{-2}$). We assign the 530.6 eV component to an O²⁻-like species.

On further exposure to oxygen (200 langmuir) the very low binding energy peak at 527.4 eV is not present and the main O(1s) intensity has shifted to higher binding energy (533.3 eV), a feature assigned to a peroxo-type species O₂^{δ-}. The concentration of the latter is calculated to be $2.44 \times 10^{15} \text{ cm}^{-2}$ oxygen atoms (or $1.22 \times 10^{15} \text{ cm}^{-2}$ O₂^{δ-} species).

We have based our assignments of the O(1s) peaks, namely, O^{δ-} (531.6 eV), O²⁻ (530.6 eV), and O₂^{δ-} (533.3 eV), on the observed reactivity of CO and CO₂ used as molecular probes of the chemical reactivity of oxygen states at cesium surfaces.³ The following reactions were observed:



We believe that these chemical reactivity arguments allow a more unambiguous identification of oxygen species than those reported elsewhere.^{4,13} A weak feature at ca. 527 eV binding energy is occasionally seen in our O(1s) data (see for example Figure 2(d)). The irreproducibility of this feature, which is absent from most of our spectra, leads us to question its assignment¹³ to an O²⁻ species. We have observed a more intense 527 eV feature when we oxidize cold-deposited amorphous Cs films,¹⁴ and we suggest it may arise from a highly electronegative oxygen species in a defective oxide.

Also shown in Figure 2(f) is an O(1s) spectrum taken at a takeoff angle (with respect to the surface normal) of $\phi = 75^\circ$ and which can be compared with spectrum e taken at a takeoff

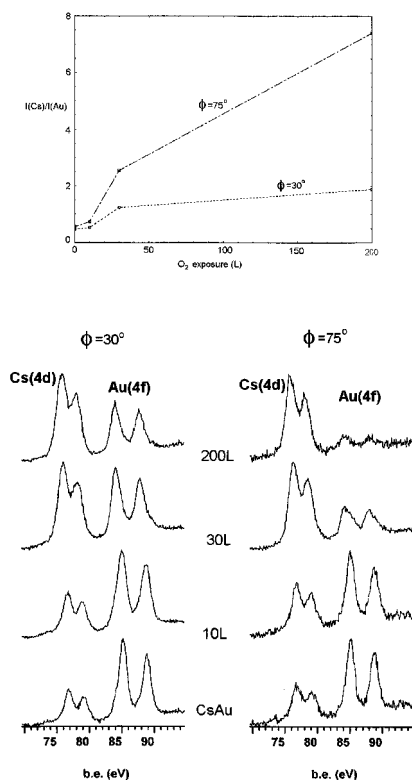


Figure 3. Au(4f) and Cs(4d) spectra for a CsAu film ($d_{\text{CsAu}} = 25 \text{ \AA}$) exposed to oxygen at 298 K at takeoff angles (with respect to the surface normal) $\phi = 30^\circ$ and $\phi = 75^\circ$. The inset shows the change in the relative intensity of Cs(4d) with respect to Au(4f) with oxygen exposure for the two different values of ϕ .

angle $\phi = 30^\circ$. Clearly the *relative intensities* of the two peaks have changed with the intensity of the lower binding energy peak increasing compared with that at high binding energy (the ratio increasing from 0.37 to 0.50) as the angle ϕ is increased. The larger is the angle ϕ (with respect to the surface normal) the more surface sensitive are the spectra, which suggests that the oxide layer is not homogeneous, O^{2-} species being preferentially situated toward the surface of the oxidized alloy film.

The Au(4f) spectra (Figure 2) also change quite dramatically with oxygen exposure at 298 K, the alloy surface becoming more goldlike with the extent of oxidation. Clearly the Au–Cs bonds are being broken, with the preferential formation of cesium oxides; in other words, dealloying has occurred.⁴ Oxygen interaction at low temperatures (80 K) also results in dealloying, which reflects the low activation energy for the process, although this is not complete at this temperature.

The atomic spatial arrangement within the oxide overlayer present at 298 K has been investigated through monitoring the angular dependence of the Cs(4d) and Au(4f) relative intensities. This is shown in Figure 3 as a function of oxygen exposure for two different angles ϕ ; there is essentially no difference with the clean CsAu films between the relative intensities of the Cs(4d) and Au(4f) peaks for ϕ values of 30° and 75° (Figure 3). However, with “oxidation” (oxygen exposures increasing from 10 langmuir to 200 langmuir) there is an increase in the Cs(4d) intensity relative to the Au(4f) intensity. This is obvious from the raw spectra but is also shown in the inset (Figure 3) in the form of a plot of the ratio of the intensities $I(\text{Cs})/I(\text{Au})$ against oxygen exposure. We therefore suggest that cesium oxide tends to segregate at the surface of the alloy film with the O(1s) angular dependent data indicating that within the oxide the peroxo-type species $\text{O}_2^{\delta-}$ lie below the O^{2-} -type oxide layer.

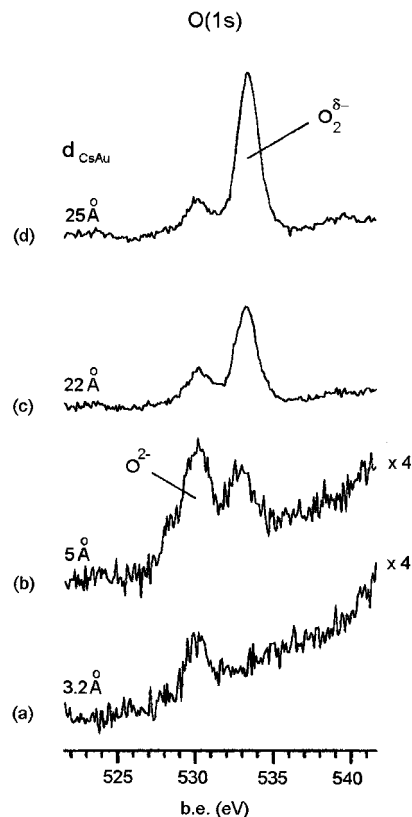


Figure 4. O(1s) spectra at the saturation coverage of oxygen at 298 K on different CsAu film thickness: (a) $d_{\text{CsAu}} = 3.2 \text{ \AA}$, (b) $d_{\text{CsAu}} = 5.0 \text{ \AA}$, (c) $d_{\text{CsAu}} = 22 \text{ \AA}$, (d) $d_{\text{CsAu}} = 25 \text{ \AA}$.

When we consider the formation of oxide species for various alloy film thickness (3.2, 5.0, 22, and 25 Å), we see (Figure 4) the preferential formation of the high O(1s) binding feature at 533.3 eV with the thicker alloy film. All the O(1s) spectra correspond to high oxygen (saturation) exposures (≥ 200 langmuir). For the thinnest film investigated (3.2 Å) the only oxygen species present is that with the low binding energy (530.3 eV) and assigned as O^{2-} . The peroxo $\text{O}_2^{\delta-}$ species only emerge after the initial formation of O^{2-} species and are, therefore, likely to be present as a result of stabilization at the oxide surface. Whether what effectively happens is a transformation of one oxygen state to another through dimerization, as we have reported in the oxidation of zinc surfaces,¹⁵ we are not able to say from the available data.

Adsorption of Carbon Monoxide. The reactivity of the oxygen states present at the CsAu alloy (25 Å) surface has been studied using carbon monoxide as the probe molecule; valuable information using this approach has been reported recently³ for oxidized cesium films. In Figure 5 is shown the O(1s) spectrum for an oxidized (30 langmuir) alloy surface; two components are present, the major one, O^{2-} (a), at 530.6 eV corresponding to a concentration of $1.45 \times 10^{15} \text{ atoms cm}^{-2}$. The minor component is at a binding energy of 531.6 eV, corresponding to a concentration of $0.75 \times 10^{15} \text{ atoms cm}^{-2}$ and is attributed to the monatomic $\text{O}^{\delta-}$ species. After exposure (100 langmuir) to carbon monoxide at 298 K, the O(1s) signal both increases in intensity and broadens, and a C(1s) feature develops at 289.3 eV. Curve fitting the broad O(1s) feature reveals two components, one at 530.6 eV and the other at 531.8 eV. The oxygen atom concentrations corresponding to these are $1.45 \times 10^{15} \text{ cm}^{-2}$ and $1.05 \times 10^{15} \text{ cm}^{-2}$, respectively. The carbon atom concentration calculated from the C(1s) intensity at 289.3 eV is $0.4 \times 10^{15} \text{ cm}^{-2}$, which gives a C:O atom ratio (based on the O(1s) intensity at 531.8 eV) of $\sim 2.7:1$, indicating the

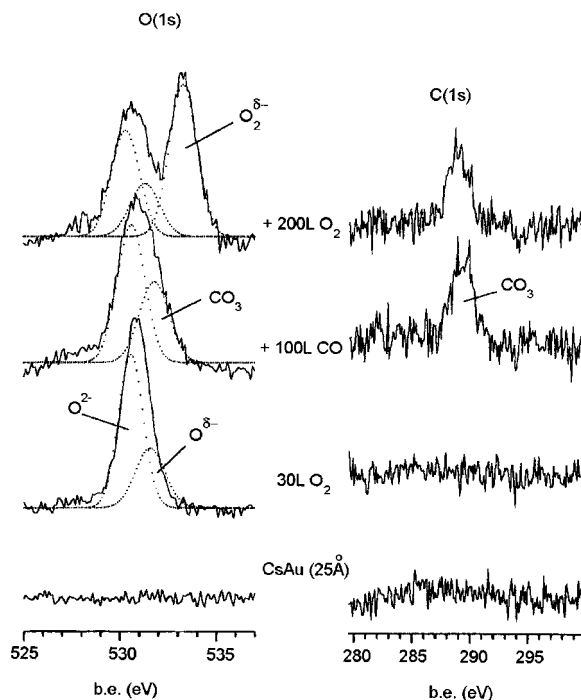
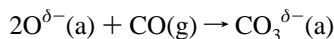


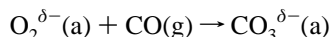
Figure 5. O(1s) and C(1s) spectra for a CsAu film (25 Å) exposed to 100 langmuir CO after exposure to 30 langmuir O₂ at 298 K. The CO dosed surface was further exposed to 200 langmuir O₂ at 298 K.

formation of surface carbonate



Exposure of this (carbonate-like) surface to dioxygen leads to the development of the high binding energy peroxo species, O(1s) at 533.3 eV, but no change to the C(1s) peak at 289.3 eV (Figure 5). Clearly the surface at this stage can stabilize oxygen in a peroxo-type state, O₂^{δ-}(a).

For a more heavily "oxidized" CsAu surface (oxygen exposure ~200 langmuir at 298 K), the reactivity to carbon monoxide (Figure 6) is somewhat analogous, with a C(1s) peak developing at 288.9 eV. The carbon atom concentration calculated from this intensity is $0.1 \times 10^{15} \text{ cm}^{-2}$. The O(1s) intensity at 533.3 eV decreased but was accompanied by both an increase and broadening of the O(1s) intensity at about 530.5 eV; we have curve fitted this to reveal two components at 530.3 and 530.7 eV. We suggest these two components are due to the presence of O²⁻ and CO₃ species, respectively. The oxygen atom concentrations calculated from the intensities of these two O(1s) peaks are 0.96×10^{15} and $0.27 \times 10^{15} \text{ cm}^{-2}$, respectively. The latter is close to three times the carbon concentration calculated from the C(1s) intensity at 288.9 eV, further supporting its assignment to a carbonate species formed through the following reaction:



Coadsorption of Carbon Monoxide and Oxygen at 298 K.

K. When a CsAu (25 Å) film was exposed (1000 langmuir) to a carbon monoxide-dioxygen (3:1) mixture the O(1s), C(1s) and Au(4f) spectra are as shown in Figure 7. In the O(1s) spectral region there emerges an intense peak at 531 eV, and there is also the feature at 533.3 eV characteristic of the "oxidized" surface (Figure 7). An intense C(1s) peak also develops at 289.3 eV, and the Au(4f) spectra suggest that there is little evidence for the presence of the CsAu component (i.e., dealloying had taken place). The carbon atom concentration corresponding to

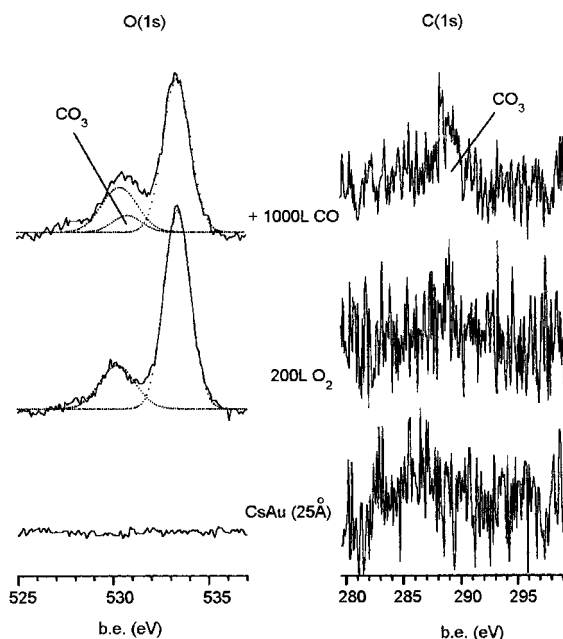
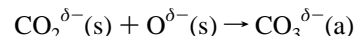
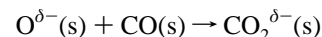
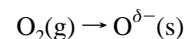
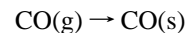


Figure 6. O(1s) and C(1s) spectra for a CsAu film (25 Å) exposed to 1000 langmuir CO at 298 K after preexposure to 200 langmuir O₂ at 298 K.

the C(1s) peak is calculated to be $0.9 \times 10^{15} \text{ cm}^{-2}$, which when compared with the oxygen atom concentration of $3.3 \times 10^{15} \text{ cm}^{-2}$ estimated from the O(1s) intensity at 531 eV gives an oxygen:carbon atom ratio of 3.7:1. This suggests the formation of both surface carbonate and oxide O²⁻ species. In addition there is the intense O(1s) peak at 533.3 eV which we can assign with confidence as the peroxo-type species O₂^{δ-}.

Therefore, the exposure of the oxidized CsAu alloy to a 3:1 mixture of carbon monoxide and oxygen leads to the formation of a surface carbonate and peroxo-type species, accompanied by complete dealloying of the CsAu film. When the carbon monoxide mixture is made richer in carbon monoxide (CO:O₂ ratio 60:1), only surface carbonate is formed (Figure 7), characterized by an O(1s) peak at 530.6 eV and a C(1s) peak at 289.1 eV. The oxygen and carbon atom concentrations are 2.4×10^{15} and $0.6 \times 10^{15} \text{ cm}^{-2}$, respectively, which can be accounted for by mainly CO₃ species but also some oxidic O²⁻ species. The Au(4f) spectra indicate that dealloying is not complete; curve fitting indicates a mixture of pure Au and the CsAu alloy. There is no evidence for a peroxo-type oxygen species with the mixture when it is very rich in CO.

We suggest that the chemistry is controlled by the oxygen adatoms formed in the dissociative chemisorption of dioxygen (see below) with the oxygen adatoms being scavenged by the excess carbon monoxide to generate surface carbonate. The pathway to peroxo species is therefore less likely under such conditions, the surface becoming totally carbonated:



This surface carbonate is also an effective barrier to further oxidation and therefore dealloying is incomplete compared with the 3:1 carbon monoxide–oxygen mixture (Figure 7).

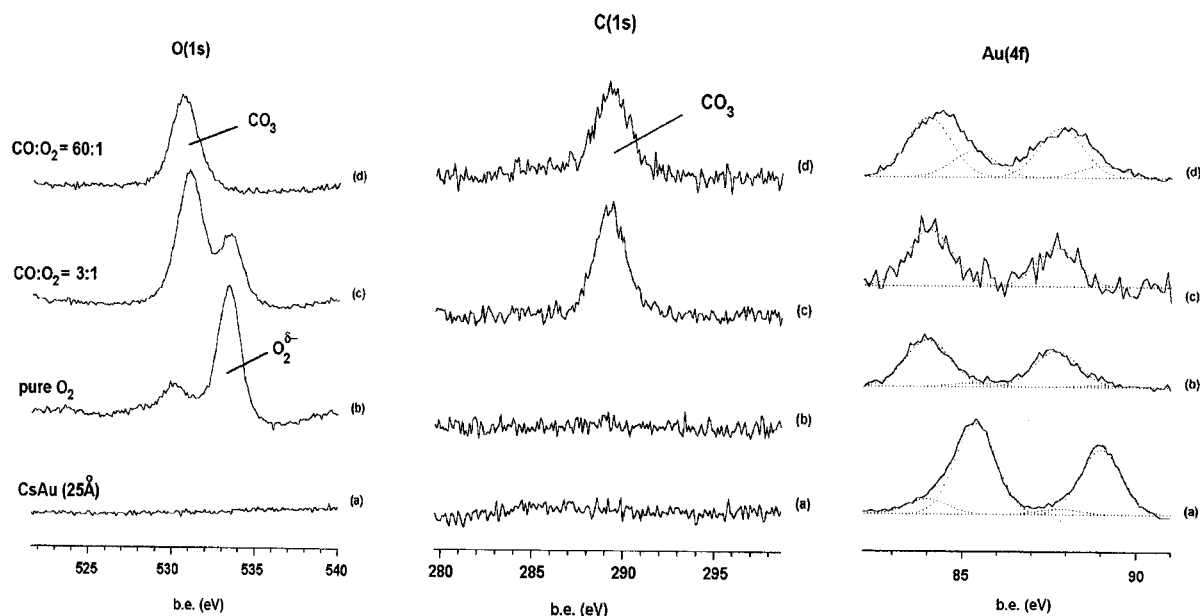


Figure 7. O(1s), C(1s), and Au(4f) spectra for a CsAu film (25 Å) (curves a) exposed to (curve b) pure oxygen (200 langmuir) and to CO–O₂ mixtures of two different compositions at 298 K (c) CO:O₂ = 3:1 (1000 langmuir) and (d) CO:O₂ = 60:1 (10 000 langmuir).

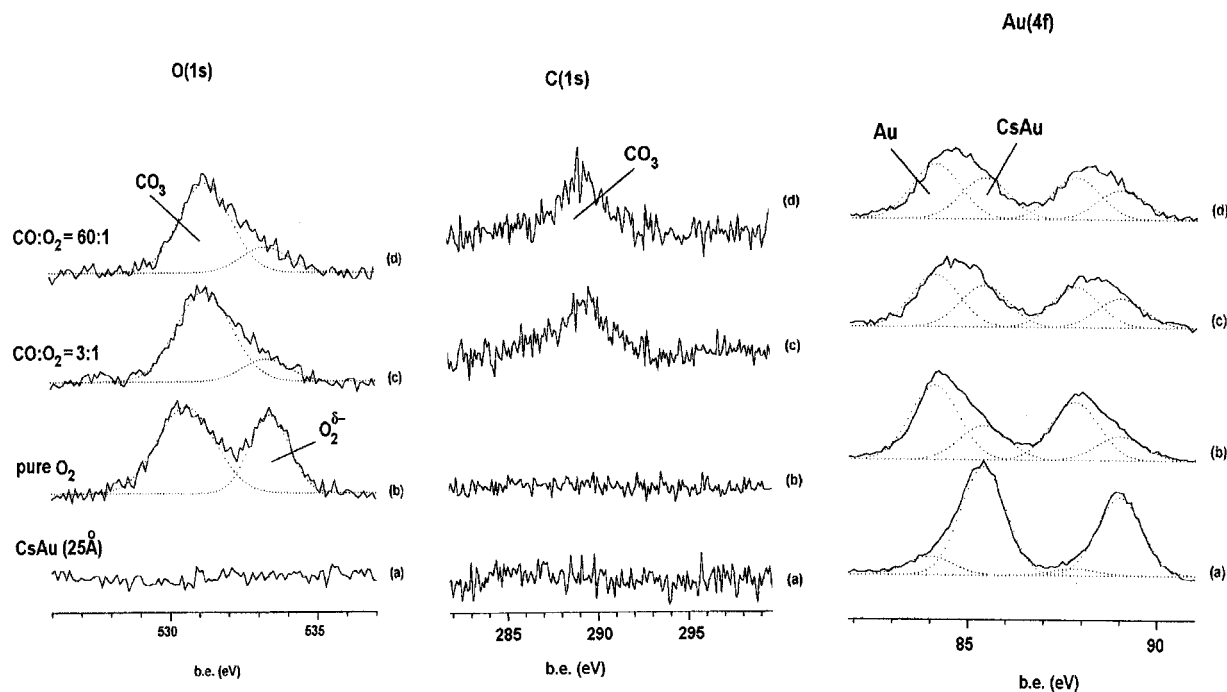


Figure 8. O(1s), C(1s), and Au(4f) spectra for a CsAu film (25 Å) (curves a) exposed to (curve b) pure oxygen (20 langmuir) and to CO–O₂ mixtures of two different compositions at 80 K (curve c) CO:O₂ = 3:1 (200 langmuir) and (curve d) CO:O₂ = 60:1 (1000 langmuir).

Coadsorption of Carbon Monoxide and Oxygen at 80 K.

Similar coadsorption studies were carried out at 80 K and the results compared with “oxidation” at the same temperature. In Figure 8 are shown O(1s), C(1s), and Au(4f) spectra for the CsAu film (25 Å) at 80 K, after oxygen interaction at 80 K and exposure to two carbon monoxide–oxygen mixtures (3:1 and 60:1).

At 80 K, pure oxygen generates two O(1s) peaks at 530.3 and 533.3 eV, assigned to oxide and peroxo-type species, O²⁻ and O₂^{δ-}. The corresponding Au(4f) spectra indicate that dealloying is incomplete at this temperature.

Exposure of the CsAu film to a 3:1 carbon monoxide–oxygen mixture resulted in an intense but broad O(1s) peak at 530.6 eV and with C(1s) intensity at 289.3 eV. The oxygen and carbon atom concentrations calculated from the O(1s) and C(1s)

spectra were 1.1×10^{15} and $0.35 \times 10^{15} \text{ cm}^{-2}$, respectively. The Au(4f) spectra indicate only partial dealloying (Figure 8).

The broad O(1s) peak can be curve-fitted to two components, a major one at 531.2 eV and a minor one at 533.3 eV; each of these correspond to oxygen atom concentrations of 0.9×10^{15} and $0.2 \times 10^{15} \text{ cm}^{-2}$, respectively. We assign the 531.2 and 289.3 eV peaks to surface carbonate with the concentrations of oxygen ($0.9 \times 10^{15} \text{ cm}^{-2}$) and carbon ($0.35 \times 10^{15} \text{ cm}^{-2}$), being close to the expected 3:1 ratio.

The O(1s), C(1s), and Au(4f) spectra when the CsAu film was exposed to a 60:1 carbon monoxide–oxygen mixture were very similar to those for the 3:1 mixture (Figure 8). In both cases oxide O²⁻ species were absent, and the peroxo species present only as a minor component.

Conclusions

Three different oxygen species can exist at 298 K on CsAu surfaces, O₂²⁻, O₂^{δ-}, and O^{δ-}, with the peroxo species being the major one at high oxygen exposure. A dimerization mechanism¹⁵ may account for the peroxo species. The oxidized alloy surface is reactive toward carbon monoxide, leading to carbonate formation. Coadsorption of carbon monoxide and oxygen result in O₂²⁻, O₂^{δ-}, and CO₃ species at 298 K with a 3:1 (CO:O₂) mixture. However, with a mixture much richer in carbon monoxide, (60:1) only oxide O^{δ-} and carbonate CO₃^{δ-} species are formed. At 80 K, both mixtures (3:1 and 60:1) result in peroxo and carbonate species, with no evidence for the low binding energy O^{δ-} species. In this case oxygen adatoms formed in the dissociation of dioxygen are routed efficiently along the carbonate pathway through interaction with carbon monoxide. The peroxo-type species O₂^{δ-} is stabilized at both the oxide overlayer and carbonate surface, its concentration increasing with the extent of oxide present at the CsAu alloy surface. For thin (~3 Å) CsAu films no peroxo species are present.

The CsAu alloy undergoes dealloying during the chemisorption of oxygen and carbon monoxide-oxygen mixtures, the process being followed through monitoring the Au(4f) spectra. Angular dependent studies of the Au(4f) and Cs(3d) spectra during oxygen chemisorption have also provided information on the segregation of cesium oxide at the surface of the alloy and on the relative spatial arrangements of the peroxo O₂^{δ-} and oxide O^{δ-} species.

Acknowledgment. We are grateful to EPSRC for their support through a ROPA Award to A.K.S.

References and Notes

- (1) Bonzel, H. P. *Surf. Sci. Rep.* **1988**, 8, 43.
- (2) Carley, A. F.; Roberts, M. W.; Strutt, A. J. *J. Phys. Chem.* **1994**, 98, 9175.
- (3) Kulkarni, G. U.; Laruelle, S.; Roberts, M. W. *Chem. Commun.* **1996**, 9; *J. Chem. Soc., Faraday Trans.* **1996**, 92, 4793.
- (4) Rodriguez, J. A.; Hrbek, J.; Kuhn, M.; Sham, T. K. *J. Phys. Chem.* **1993**, 97, 4737.
- (5) Rodriguez, J. A.; Hrbek, J.; Yang, Y.-W.; Kuhn, M.; Sham, T. K. *Surf. Sci.* **1993**, 293, 260.
- (6) Skottke-Klein, M.; Böttcher, A.; Imbeck, R.; Kennou, S.; Morgante, A. Ertl, G. *Thin Solid Films* **1991**, 203, 131.
- (7) Wertheim, G. K.; Rowe, J. E.; Chiang, C.-M.; Malic, R. A.; Buchanan, D. N. E. *Surf. Sci.* **1995**, 330, 27.
- (8) Wertheim, G. K.; Bates, C. W., Jr.; Buchanan, D. N. E. *Solid State Commun.* **1979**, 30, 473.
- (9) Simon, A. *Structure and Bonding*; Springer-Verlag: New York, 1979; Vol. 36, p 81.
- (10) Roberts, M. W. *Chem. Soc. Rev.* **1989**, 18, 451; *Surf. Sci.* **1994**, 299/300, 769; *Chem. Soc. Rev.* **1996**, 25, 437.
- (11) Carley, A. F.; Roberts, M. W. *Proc. R. Soc. London* **1978**, A363, 403. Roberts, M. W. *Adv. Catal.* **1980**, 29, 55.
- (12) Carley, A. F.; Ph.D. Thesis, University of Bradford, 1980 and references therein.
- (13) Jupille, J.; Dolle, P.; Besançon, M. *Surf. Sci.* **1992**, 260, 271.
- (14) Carley, A. F.; Chambers, A.; Roberts, M. W.; Santra, A. K. Unpublished data.
- (15) Carley, A. F.; Rajumon, M. K.; Roberts, M. W.; Fancheng, W. *J. Solid State Chem.* **1994**, 112, 214.
- (16) 1 langmuir = 10⁻⁶ Torr s.